Non-linear photoionization in the soft X-ray regime

M. Richter[1a], S. V. Bobashev[2], A. A. Sorokin[1,2], K. Tiedtke[3]

[1]*Physikalisch-Technische Bundesanstalt, Abbestraße 2-12, 10587 Berlin, Germany*

[2]*Ioffe Physico-Technical Institute, Polytekhnicheskaya 26, 194021 St. Petersburg, Russia*

[3]*Deutsches Elektronen-Synchrotron, Notkestraße 85, 22603 Hamburg, Germany*

At the new Free-electron LASer in Hamburg FLASH, we have studied photon-matter interaction by means of ion time-of-flight spectroscopy on gases in the soft X-ray regime. Emphasis was laid on the quantitative investigation of non-linear effects upon photoionization by the highly intense soft X-ray laser pulses. In the photon energy range from 38 to 93 eV, we have observed non-linearities due to space-charge effects, target depletion, and sequential and direct multi-photon ionization at irradiance levels of up to 10^{16} W cm^{-2}. The work is related to the development of photon diagnostic tools that are based on gas-phase photoionization for current and future X-ray laser facilities but might be of significance for any experiment at fourth generation light sources.

PACS numbers: 32.80.Rm, 32.80.Fb, 06.30.-k

[a] mathias.richter@ptb.de (E-mail), +49 30 6392 5084 (Phone), +49 30 6392 5084 (Fax)

Introduction

Recent progress in the development of X-ray lasers [1-3] has opened the doorway to totally new experiments of materials research on nanometer and femtosecond scales. Based on Higher-Harmonics Generation (HHG) or Free-Electron Laser (FEL) technique, the strong X-ray pulses with femtosecond pulse duration will allow in the near future to study ultra-fast processes, e.g., on surfaces or within biological systems [4-6]. However, photon-matter interaction at ultra-high intensities is affected by non-linear processes as known from optical radiation [7,8]. At short wavelengths, non-linear dynamics even represent a largely unknown territory. It concerns, in particular, the photoelectric effect by highly intense X-rays. Therefore, we have studied at the new Free-electron LASer in Hamburg FLASH [2,3] atomic and molecular photoionization from a fundamental point of view [9-12]. In continuation of former work in the vacuum ultraviolet [13-18], we have quantitatively investigated space-charge effects, saturation due target depletion, sequential and direct multi-photon ionization, and strong-field phenomena in the soft X-ray regime. Thus, also the limits for the application of gas-ionization detectors for the characterization of X-ray lasers were explored [19,20]. Our experiments of quantitative ion Time-Of-Flight (TOF) mass/charge spectroscopy were performed at the wavelengths of 32.6 nm, 29.0 nm, and 13.3 nm, i.e. at the photon energies of 38.0 eV, 42.8 eV, and 93 eV. The FLASH pulse duration was in the range from 10 to 25 fs. At the photon energy of 93 eV, we have achieved, e.g., irradiance levels of up to 10^{16} W cm^{-2} with the aid of an Extreme Ultra-Violet (EUV) multilayer mirror [21]. Our work on free atoms and molecules refers to the fundamental aspects of photon-matter interaction but might be of significance for any investigation at current and future X-ray laser facilities on fields like plasma physics, new materials, femtochemistry, and biochemical structure and dynamics.

1 Experimental set-up

Fig. 1 shows schematically the apparatus used at the microfocus beamline BL2 at FLASH [9]. It consists of a vacuum chamber homogeneously filled with the almost transparent target gas at a pressure in the range from 10^{-4} Pa to 10^{-2} Pa, an ion TOF spectrometer movable along the photon beam by ± 2 cm around the focus position, and a Gas-Monitor Detector (GMD) [19] about 50 cm behind the focus for the online measurement of the absolute FEL pulse energy of up to 20 μJ with a relative standard uncertainty of 10%. Calibration of the GMD was performed at the electron storage ring BESSY II in the laboratory of the Physikalisch-Technische Bundesanstalt (PTB) [22,23]. Ions generated within the BL2 focus of 15 μm in diameter (FWHM) are extracted by a homogeneous electric field parallel to the polarization axis of the 100% polarized photon beam. Having passed the entrance slit with a width of 1 mm in photon beam direction and a drift section, the ions are detected by an open electron multiplier optimized and tested for high linearity from 1 to 10^6 ions detected per FEL pulse without saturation. During measurement, ion TOF and GMD single-shot signals are recorded simultaneously by means of a digital oscilloscope using the FEL bunch clock for triggering.

2 Space-charge effects

Fig. 2 shows three single-shot ion TOF spectra of neon taken at 38-eV photon energy in the focus of BL2. The high resolution spectrum (a) was measured at the extremely low FEL pulse energy of 3.7 nJ so that only 750 ions were generated during the first photon pulse. This spectrum is not affected by any space-charge effect and reflects the resolution of our ion TOF spectrometer which is better than 1%. The broadened spectra labeled (b) and (c), on the other hand, were obtained at pulse energies above 3 μJ so that 150,000 (b) and 420,000 ions (c) were generated per pulse, respectively. Here, up to 50% of the atoms within the interaction

volume were ionized by the photon pulse. The strong broadening of the peaks is explained by Coulomb repulsion of the ionized targets and was found to increase almost linear with the number of ions generated per pulse. At very high ion signals, structuring of the individual ion peaks occurs (Fig. 2c) and Coulomb repulsion causes signal saturation by incomplete extraction and collection of the energetic photoions. On the other hand, by working, e.g., at sufficiently low target gas density and, thus, at high ion TOF spectrometer resolution, linearity on the ion detection was ensured. For our experimental study of inner-atomic non-linearities upon photoionization, we could also suppress any interaction arising from neighboring atoms or ions, i.e. avoid plasma effects, when working at moderate signal intensities.

3 Target depletion

If a considerable percentage of the targets within the interaction volume is ionized by a single photon pulse, a further saturation effect may occur which is due to target depletion. While for the first photons within a pulse 100% of the targets are available to be photoionized, the target number may already be strongly reduced for the last photons of a pulse which explains this type of non-linearity. In the simplified case of a rectangular beam profile, the number N_{ion} of ions generated per pulse is described by an exponential saturation function of the photon number per pulse N_{ph} [9]:

$$\frac{N_{ion}}{n\, z\, A} = 1 - \exp\left(- N_{ph} \frac{\sigma}{A} \right). \qquad (1)$$

In contrast to space-charge effects, saturation due to target depletion does not depend on the initial target gas density n but on the photoionization cross section σ and the photon beam cross section A only. z is the length of the interaction volume along the photon beam. Fig. 3

shows an example of such saturation curve we have obtained on neon atoms at the photon energy of 38.0 eV. The effect was used as a new method to derive the photon beam cross section *A* and, by that, focus size and beam waist at BL2 [9]. For this purpose, the absolute photon number per pulse was measured with the aid of our calibrated GMD and the measured saturation curves were fitted by Eq. 1, using the known one-photon single ionization cross section of neon $\sigma(38.0\ \text{eV}) = (8.6 \pm 0.3) \times 10^{-18}\ \text{cm}^2$ [24].

4 Sequential multi-photon ionization

If a considerable percentage of the targets within the interaction volume is ionized by a single photon pulse, the generated ions also represent a new sort of targets which can be further ionized within the same pulse. In particular, sequences of one-photon ionization processes may occur as long as the photon pulse duration is short enough so that the atomic and ionic targets may be regarded to be frozen. This type of sequential multi-photon ionization is restricted to photon energies above the respective ionization thresholds and, hence, not possible in the optical regime. As an example, sequential two-photon double ionization:

$$\mathrm{X} \xrightarrow{\text{1st photon}} \mathrm{X}^{1+} \xrightarrow{\text{2nd photon}} \mathrm{X}^{2+} \tag{2}$$

was studied at FLASH firstly on molecular nitrogen at the photon energy of 38.0 eV [10] and later on neon atoms in the same spectral range [11]. Solving the rate equations for generation and annihilation of the different atomic and ionic species, results in a X^{2+} to X^{1+} ion yield ratio within the regime free from any target depletion [11,25]:

$$\frac{N_{2+}}{N_{1+}} = \frac{\sigma^{(1)}_{1+\rightarrow 2+}}{2} H_{ph}, \tag{3}$$

i.e. a linear increase with the photon exposure $H_{ph} = N_{ph} / A$. $\sigma^{(1)}_{1+\rightarrow 2+}$ denotes the one-photon single ionization cross section of X^{1+} leading to X^{2+}. For neon (X = Ne), Fig. 4a shows a corresponding experimental result which was obtained at the photon energy of (42.8 ± 0.2) eV, i.e. well above the threshold for the $Ne^{1+} \rightarrow Ne^{2+}$ process at 41.0 eV [26]. Fitting the initial slope of the experimental data with the linear function of Eq. 3, yields $\sigma^{(1)}_{1+\rightarrow 2+}$(42.8 eV) = (7.0 ± 1.0) × 10^{-18} cm^2 as a fit parameter which is in fair agreement with results obtained from a Ne^+ ion beam photoionization experiment using synchrotron radiation [27]. However, the latter comparison is difficult to perform because there is a number of resonances in Ne^+ around 42.8 eV which are partly covered by the 1% spectral bandpass of the FLASH photon beam [2,3].

A sequence of two one-photon ionization processes as expressed by Eq. 2 may alternatively be regarded and theoretically described as a $X \rightarrow X^{2+}$ two-photon double ionization via a real intermediate X^{1+} state. Perturbation theory yields for the rate of a m(=2)-photon process outside the saturation regime [7]:

$$\dot{N}^{(m)} = n\, z\, A\, \sigma^{(m)} \left(\frac{E}{\hbar\omega} \right)^m \tag{4}$$

with the irradiance E:

$$E = \frac{\hbar\omega\, N_{ph}}{A\, \Delta t} = \frac{\hbar\omega\, H_{ph}}{\Delta t}. \tag{5}$$

$\sigma^{(m)}$ denotes the m-photon ionization cross section, $\hbar\omega$ the photon energy, and Δt the FEL pulse duration. As a result, one obtains for the X^{2+} to X^{1+} ratio:

$$\frac{N_{2+}}{N_{1+}} = \frac{\sigma_{2+}^{(2)}}{\sigma_{1+}^{(1)}} \frac{E}{\hbar\omega} = \frac{\sigma_{2+}^{(2)}}{\sigma_{1+}^{(1)}} \frac{H_{ph}}{\Delta t}. \quad (6)$$

Comparison of Eq. 6 with Eq. 3 leads to an expression for the sequential two-photon double ionization cross section:

$$\sigma_{2+}^{(2)} = \sigma_{1+}^{(1)} \sigma_{1+\rightarrow 2+}^{(1)} \frac{\Delta t}{2} \quad (7)$$

being composed of the two one-photon single ionization cross sections for the first and the second step of the sequence in Eq. 2, respectively. In the case of neon, one obtains with our experimental result for $\sigma_{1+\rightarrow 2+}^{(1)}(42.8\ \text{eV}) = (7.0 \pm 1.0) \times 10^{-18}\ \text{cm}^2$, the literature value for $\sigma_{1+}^{(1)}(42.8\ \text{eV}) = (8.2 \pm 0.3) \times 10^{-18}\ \text{cm}^2$ [24], and the estimated value for $\Delta t = (25 \pm 5)$ fs [2], a sequential two-photon double ionization cross section of $\sigma_{2+}^{(2)}(42.8\ \text{eV}) = (7.2 \pm 2.5) \times 10^{-49}$ cm^4s [11].

However, treating two subsequent one-photon processes (Eq. 2) as a two-photon process via a long-living intermediate state is a little artificial. This is also reflected by the cross section for such a two-photon process depending on the duration Δt of the photon pulse (Eq. 7). The latter is due to the irradiance E being the key quantity of the radiation field on the description of real multi-photon processes (Eq. 4). E decreases inversely with increasing pulse duration Δt (Eq. 5) while, on the other hand, a sequential two-photon process depends on the photon exposure H_{ph} only and, thus, not on Δt (Eq. 3). On the construction of a sequential two-photon double ionization cross section, this circumstance leads to its linear increase with Δt as expressed by Eq. 7.

5 Direct multi-photon ionization

A direct two-photon process, i.e. via a virtual instead of a real intermediate state, was observed in the soft X-ray regime firstly on the double ionization of helium (He) using a HHG source at 41.8 eV photon energy [15,16]. Fig. 5 shows, however, our results of ion TOF spectroscopy we have obtained on He with 42.8 eV photons at FLASH. The He^{2+} generation clearly decreases in intensity with respect to the linear He^{1+} one-photon process when moving our set-up out of the BL2 focus (Fig. 5b), i.e. increasing the photon beam cross section *A* and, hence, reducing the mean irradiance *E* (Eq. 5). This behavior indicates the He^{2+} signal being dominated by non-linear multi-photon ionization as described by Eq. 4. In particular, the linear increase of the He^{2+} to He^{1+} ion yield ratio with irradiance as demonstrated by Fig. 4c identifies the He^{2+} generation as a two-photon process (see, e.g., Eq. 6). He^{2+} generation arising from one-photon double ionization by higher FEL harmonics at higher photon energies [28] whose contributions do not vary along the photon beam, obviously, plays a negligible role.

However, the He^{1+} and He^{2+} ionization energies, starting from He, amount to 24.6 and 79.0 eV, respectively [26]. Hence, the $He^{1+} \rightarrow He^{2+}$ process requires at least (79.0 – 24.6) eV = 54.4 eV. At the photon energy of 42.8 eV, the He^{2+} signal in Fig. 5 can therefore not be explained by a sequential two-photon process via He^{1+} as discussed for neon but must be due to the direct two-photon double ionization $He \rightarrow He^{2+}$. Fitting the measured data for the He^{2+} to He^{1+} ratio as shown in Fig. 4c by a linear function of irradiance according to Eq. 6 and using the known one-photon single ionization cross section $\sigma_{1+}^{(1)}(42.8\ \text{eV}) = (2.75 \pm 0.08) \times 10^{-18}$ cm^2 [24], we obtain the experimental result for the direct two-photon double ionization cross section of helium of $\sigma_{2+}^{(2)}(42.8\ \text{eV}) = (1.6 \pm 0.6) \times 10^{-52}$ cm^4s [11]. This value agrees fairly

well with the estimation of 10^{-52} cm^{4}s derived from the HHG measurements at 41.8 eV photon energy [16]. Both values perfectly lie in between the two main groups of theoretical predictions for this cross section [29-33] as demonstrated by Fig. 6. However, comparing these data with our results for neon ($\sigma_{2+}^{(2)}$ (42.8 eV) = (7.2 ± 2.5) × 10^{-49} cm^{4}s), leads to the conclusion that within the soft X-ray regime, using FEL pulses of tenths of femtoseconds in pulse duration, direct multi-photon processes are much weaker than sequential multi-photon processes, i.e. sequences of one-photon processes via long-living intermediate states.

Since the strength of direct multi-photon ionization depends on the irradiance E (Eq. 4) and, hence, also on the pulse duration Δt (Eq. 5) the latter may be experimentally determined by means of autocorrelation technique [15]. Splitting an FEL pulse with the temporal pulse shape $f(t)$ into two parts with the irradiance amplitudes E_1 and E_2 and a temporal delay of t'($E(t) = E_1\ f(t) + E_2\ f(t\text{-}t')$), one obtains according to Eq. 4 for a direct two-photon process:

$$\frac{N^{(2)}(t')}{N^{(2)}(t' \to \infty)} = 1 + \alpha \int_{-\infty}^{+\infty} f(t)\, f(t-t')\, dt, \qquad \alpha = \frac{2E_1E_2}{E_1^2 + E_2^2}. \tag{8}$$

At FLASH, the determination of the pulse shape function $f(t)$ and, by that, the pulse duration is scheduled to be realized in 2008 by investigating the direct two-photon double ionization of helium as a function of the pulse delay t', using a two-pulse correlator for the pulse splitting [34] and evaluating the convolution integral in Eq. 8.

6 Strong-field phenomena

Direct multi-photon ionization may also be part of a more complex photoionization sequence. On neon atoms, e.g., we have observed a four-photon process, starting with a sequential two-photon double ionization leading via Ne^{1+} to Ne^{2+} (Eq. 2) followed by a direct two-photon transition from Ne^{2+} to Ne^{3+} [11]. In the last step, the Ne^{2+} ions may be regarded as the targets for the two-photon process. As a result, the Ne^{3+} to Ne^{2+} ion yield increases with the square of irradiance, according to Eq. 4, which is experimentally confirmed by Fig. 4b. Even more complex is the situation at higher photon energy and irradiance. With the help of a spherical Extreme-Ultra-Violet (EUV) multilayer mirror [21], we have realized at FLASH a focal spot of 3 μm in diameter at a wavelength of 13.3 nm, i.e. the photon energy of 93 eV [12]. At irradiance levels of up to about 10^{16} W cm^{-2}, we investigated the photoionization of xenon (Xe) atoms and observed very high degrees of ionization as demonstrated by Fig. 7. For the generation of Xe^{21+}, e.g., a total photon energy of more than 5 keV must have been absorbed during a single photon pulse of 10 fs duration [3], i.e. more than 57 EUV photons [35]. Within the scheme of a photoionization sequence, at least 19 steps of one- to seven-photon transitions are required to reach a Xe^{21+} state starting from neutral Xe in its ground state. Hence, the situation might be beyond the multi-photon scheme and perturbation theory.

Within the regime of optical femtosecond lasers, in fact, photon-matter interaction is often described by treating intense light as an electromagnetic wave of high field strength which strongly influences the atomic electron structure [7,8,35]. Validity of this wave picture of light depends on the ponderomotive energy U_p which is the quiver energy transferred to a free electron by the oscillating field. U_p increases linearly with the irradiance E, but decreases with the square of the photon energy $\hbar\omega$ according to:

$$U_p / \mathrm{eV} \approx 1.44 \times \frac{E/(10^{13}\ \mathrm{W\ cm^{-2}})}{(\hbar\omega / \mathrm{eV})^2} \tag{9}$$

and defines the so-called Keldysh parameter [36]:

$$\gamma = \sqrt{\frac{I}{2\,U_p}} \tag{10}$$

with the ionization energy I of the target (= 12.1 eV for Xe). Using, e.g., a titan-sapphire femtosecond laser at $E = 10^{16}$ W cm^{-2} in the optical regime at the wavelength of 800 nm [35], i.e. $\hbar\omega$ = 1.55 eV, γ amounts to 0.10 which clearly lies in the so-called non-perturbative regime ($\gamma < 1$). In our case ($E = 10^{16}$ W cm^{-2} at $\hbar\omega$ = 93 eV), however, γ = 6.0 is obtained which still suggests a perturbative description. One can, therefore, conclude that the mechanisms of photon-matter interaction are not totally clear under the conditions of ultra-high photon intensities in conjunction with high photon energies. Further experimental and theoretical efforts seem to be necessary.

Acknowledgement

The authors would like to thank T. Feigl, E. Filatova, A. Gottwald, J. R. Schneider, B. Sonntag, G. Ulm, M. Wellhöfer, H. Wabnitz, and M. Yurkov for continuous support.

References

[1] T. Sekikawa, A. Kosuge, T. Kanai, S. Watanabe: Nature **432**, 605 (2004)

[2] V. Ayvazyan *et al.*: Eur. Phys. J. D **37**, 297 (2005)

[3] W. Ackermann *et al.*: Nature Photonics **1**, 336 (2007)

[4] P. G. O'Shea, H. P. Freund: Science **292**, 1853 (2001)

[5] H. C. Kapteyn, T. Ditmire: Nature **420**, 467 (2002)

[6] J. Feldhaus, J. Arthur, J. B. Hastings: J. Phys. B **38**, S799 (2005)

[7] M. Protopapas, C. H. Keitel, P. L. Knight: Rep. Prog. Phys. **60**, 389 (1997)

[8] N. Delone, V. Krainov: *Multiphoton Processes in Atoms* (Springer, New York, 2000)

[9] A. A. Sorokin *et al.*: Appl. Phys. Lett. **89**, 221114 (2006)

[10] A. A. Sorokin, S. V. Bobashev, K. Tiedtke, M. Richter: J. Phys. B **39**, L299 (2006)

[11] A. A. Sorokin, M. Wellhöfer, S. V. Bobashev, K. Tiedtke, M. Richter: Phys. Rev. A **75**, 051402(R) (2007)

[12] A. A. Sorokin, S. V. Bobashev, T. Feigl, K. Tiedtke, H. Wabnitz, M. Richter: Phys. Rev. Lett. **99**, 213002 (2007)

[13] H. Wabnitz *et al.*: Nature **420**, 482 (2002)

[14] N. Miyamoto *et al.*: Phys. Rev. Lett. **93**, 083903 (2004)

[15] Y. Nabekawa, H. Hasegawa, E. J. Takahashi, K. Midorikawa: Phys. Rev. Lett. **94**, 043001 (2005)

[16] H. Hasegawa, E. J. Takahashi, Y. Nabekawa, K. L. Ishikawa, K. Midorikawa: Phys. Rev. A **71**, 023407 (2005)

[17] H. Wabnitz *et al.*: Phys. Rev.Lett. **94**, 023001 (2005)

[18] E. P. Benis, D. Charalambidis, T. N. Kitsopoulos, G. D. Tsakiris, P. Tzallas: Phys. Rev. A **74**, 051402(R) (2006)

[19] M. Richter *et al.*: Appl. Phys. Lett. **83**, 2970 (2003)

[20] K. Tiedtke *et al.*: J. Appl. Phys. (2008)

[21] T. Feigl, S. Yulin, N. Benoit, N. Kaiser: Microelectronic Engineering **83**, 703 (2006)

[22] R. Klein, M. Krumrey, M. Richter, F. Scholze, R. Thornagel, G. Ulm: Synchrotron Radiation News **15**, 23 (2002)

[23] A. Gottwald, U. Kroth, M. Krumrey, M. Richter, F. Scholze, G. Ulm: Metrologia **43**, S125 (2006)

[24] J. M. Bizau, F. J. Wuilleumier: J. Electron Spectrosc. Relat. Phenom. **71**, 205 (1995)

[25] P. Lambropoulos, X. Tang: J. Opt. Soc. Am. B **4**, 821 (1987)

[26] D. C. Morton: Astrophys. J., Suppl. Ser. **149**, 205 (2003)

[27] A. M. Covington *et al.*: Phys. Rev. A **66**, 062710 (2002)

[28] S. Düsterer *et al.*: Opt. Lett. **31**, 1750 (2006)

[29] L. Feng, H. W. van der Hart: J. Phys. B **36**, L1 (2003)

[30] S. Laulan, H. Bachau: Phys. Rev. A **68**, 013409 (2003)

[31] E. Foumouo, G. L. Kamta, G. Edah, B. Piraux: Phys. Rev. A **74**, 063409 (2006)

[32] L. A. A. Nikolopoulos, P. Lambropoulos: J. Phys. B **40**, 1347 (2007)

[33] I. A. Ivanov, A. S. Kheifets: Rev. A **75**, 033411 (2007)

[34] R. Mitzner, M. Neeb, T. Noll, N. Pontius, W. Eberhardt: Proc. SPIE **5920**, 59200D (2005)

[35] K. Yamakawa *et al.*: Phys. Rev. Lett. **92,** 123001 (2004)

[36] L. V. Keldysh: Sov. Phys. JETP **20**,1307 (1965)

Figure captions

FIG. 1. Schematic diagram of the experimental set-up as used for photoionization experiments on gases at the microfocus beamline BL2 at FLASH.

FIG. 2. Three single-shot ion TOF spectra of neon (Ne) obtained at 38-eV photon energy from two subsequent FEL pulses (pulse distance: 1 μs) with 750 (a), 150,000 (b), and 420,000 (c) ions generated during the first pulse, respectively.

FIG. 3. Number of Ne^+ ions created per FEL pulse from Ne atoms as a function of the photon number per pulse at the photon energy of 38.0 eV. The solid line represents a fit curve according to Eq. (1). The dashed line depicts a linear dependence for comparison [9].

FIG. 4. Ion-yield ratios as a function of mean irradiance E and photon exposure H_{ph} taken at 42.8 eV photon energy: (a) Ne^{2+} to Ne^+ ratio, (b) Ne^{3+} to Ne^{2+} ratio, and (c) He^{2+} to He^+ ratio. The data were corrected for the pulse-to-pulse statistics of the photon intensity and the relative detection efficiencies of the different ion species, respectively [11].

FIG. 5. Ion TOF spectra of helium (He) taken at 42.8 eV photon energy in the focus of BL2 at an irradiance of 4.6×10^{13} W cm^{-2} (a) and out of the focus at an irradiance of 1.1×10^{13} W cm^{-2} (b). Each spectrum represents an accumulation over hundreds of consecutive FEL shots.

FIG. 6. Two-photon double ionization cross section of helium as measured at FLASH [11] and using a HHG source [16]. The most recent theoretical predictions are shown for comparison [29-33].

FIG. 7. Ion TOF spectrum of xenon (Xe) taken at a photon energy of 93 eV and a mean pulse irradiance level of 7.8×10^{15} W cm^{-2}. In the low TOF regime (below 5 μs), the ion intensities were multiplied by a factor of 20. The multiplet structures of the different ion signals are due to the Xe isotope distribution [12].

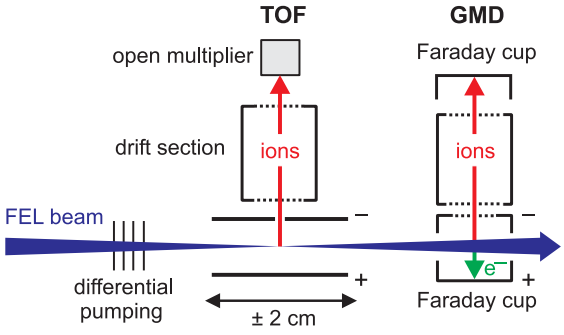

FIG. 1.

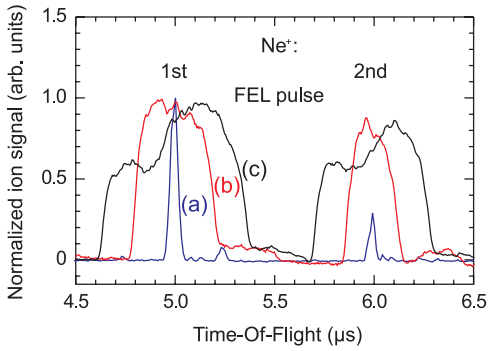

FIG. 2.

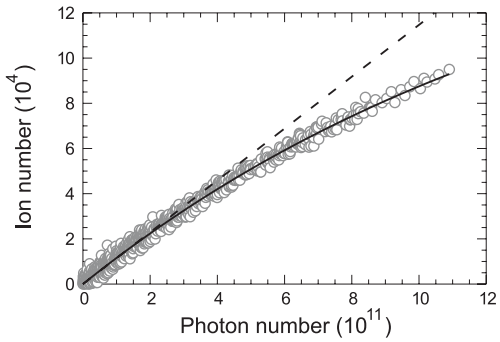

FIG. 3.

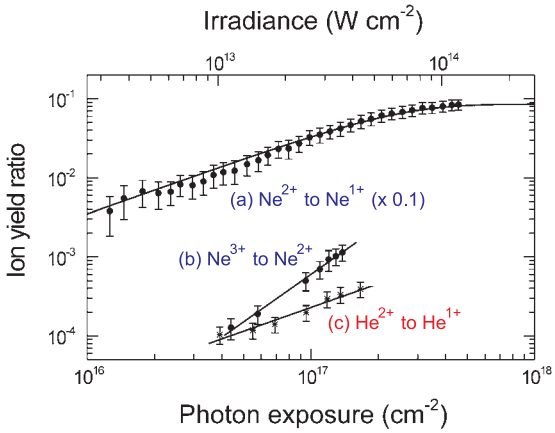

FIG. 4.

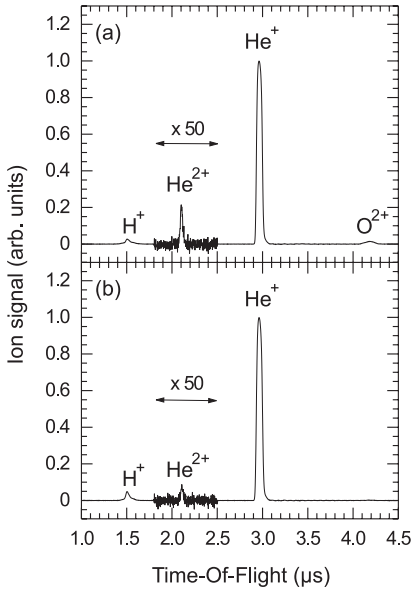

FIG. 5.

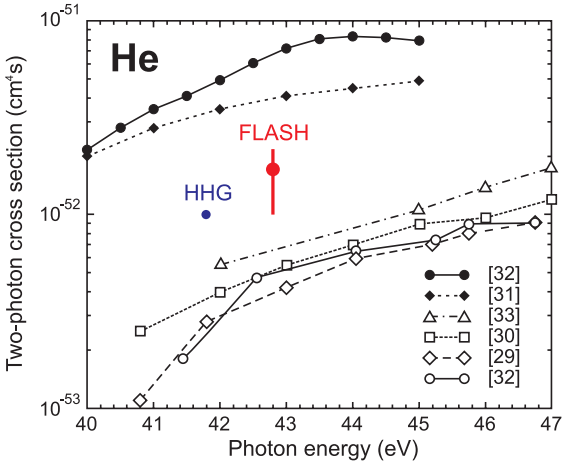

FIG. 6.

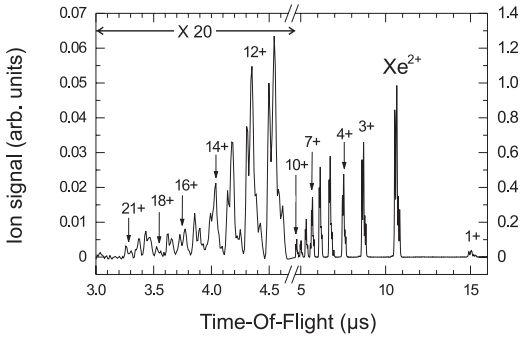
Ion signal (arb. units)
Time-Of-Flight (μs)
X 20
Xe2+
12+
14+
16+
18+
21+
10+
7+
4+
3+
1+
0.07
0.06
0.05
0.04
0.03
0.02
0.01
0
1.4
1.2
1.0
0.8
0.6
0.4
0.2
0
3.0
3.5
4.0
4.5
5
10
15

FIG. 7.